

COS Φ : Artificial Pheromone System for Robotic Swarms Research

Farshad Arvin¹, Tomáš Krajník², Ali Emre Turgut³ and Shigang Yue¹

Abstract—Pheromone-based communication is one of the most effective ways of communication widely observed in nature. It is particularly used by social insects such as bees, ants and termites; both for inter-agent and agent-swarm communications. Due to its effectiveness; artificial pheromones have been adopted in multi-robot and swarm robotic systems for more than a decade. Although, pheromone-based communication was implemented by different means like chemical (use of particular chemical compounds) or physical (RFID tags, light, sound) ways, none of them were able to replicate all the aspects of pheromones as seen in nature. In this paper, we propose a novel artificial pheromone system that is reliable, accurate and it uses off-the-shelf components only – LCD screen and low-cost USB camera. The system allows to simulate several pheromones and their interactions and to change parameters of the pheromones (diffusion, evaporation, etc.) on the fly allowing for controllable experiments. We tested the performance of the system using the *Colias* platform in single-robot and swarm scenarios. To allow the swarm robotics community to use the system for their research, we provide it as a freely available open-source package.

Index Terms—Pheromone Communication, Artificial pheromones, Autonomous Robot, Swarm Robotics, Localization

I. INTRODUCTION

Nature is one of the best sources of inspiration for solutions to different problems in different domains. Swarm robotics system [1] is such a domain in which inspiration from social behavior and coordination capabilities of social insects [2] is heavily used in controlling the robots. The success of a group in accomplishing a task relies heavily on the interactions among its members. In particular, inter-agent communication plays an important role in achieving collective behaviors. Various communication mechanisms based on physical (tactile, vibration and visual) or chemical effects (pheromones) are known to be used by social insects for inter-agent communication. Among these, pheromone-based communication is one of the most effective mechanisms that is widely utilized by the social insects [3].

Pheromone-based communication has been in use in swarm robotics both in simulation-based [4] and real-robot based studies for almost a decade [5]. In real-robot based studies, chemical substances such as alcohol are used to simulate pheromones [6], [7], [8], [9]. Although, with this approach some of the characteristics of pheromones (evaporation and diffusion) are replicated, it still lacks

This work was supported by EU FP7 projects EYE2E (269118), LIVCODE (295151), HAZCEPT (318907) and STRANDS (600623).

¹Computational Intelligence Laboratory (CIL), University of Lincoln, LN6 7TS, United Kingdom {farvin, syue}@lincoln.ac.uk

²Lincoln Centre for Autonomous Systems (L-CAS), University of Lincoln, LN6 7TS, United Kingdom tkrajnik@lincoln.ac.uk

³Mechanical Engineering Department, METU, 06800 Ankara, Turkey aturgut@metu.edu.tr



Fig. 1. Artificial pheromone system with 5 *Colias* robots, LCD screen as the pheromone-enabled ground and an external camera for robot localisation.

important features such as: being able to use multiple chemicals, difficulty in controlling evaporation and diffusion rates and chemicals being dangerous for human health. Artificial chemical pheromones also require complex and expensive sensors to be developed which renders these approaches infeasible. Therefore, the pheromones were also simulated by means of RFID tags [10], [11], audio sources [12], [13] and light sources [14], [15], [16], [17]. These methods are readily available, easy to use and very flexible when compared to the chemical counterpart. However, there are also some drawbacks, such as finite size of RFID tags limiting the resolution of the simulated pheromone trails or adjustment of the evaporation and diffusion rates of the simulated pheromone using audio signals being almost impossible. On the other hand, light shows flexible characteristics, which can be emitted with different intensities using low-cost components as presented in [17]. However, when light is used, the experiments need larger robots and arena. Garnier et al. [18] presented an experimental setup to study on pheromone-based communication with micro autonomous robots using the projected light similar to [17].

In this paper, we present a novel pheromone communication method for a swarm robotic system based on precise and fast visual localization [19]. The system allows to simulate virtually unlimited number of different pheromones and provides the result of their interaction as a gray-scale image on a horizontal LCD screen that the robots move on. In order to demonstrate the pheromone communication method, we used *Colias- Φ* autonomous micro robot as shown in Fig. 1.

When compared to the aforementioned methods, our method improves the state-of-the-art as follows: (1) High resolution and precise trails can be formed due to the high resolution LCD screen, (2) all the parameters of the pheromones (diffusion, evaporation and thickness) are

precisely controllable, (3) the system also simulates the interaction of multiple pheromones, that can amplify or suppress each other, and (4) different pheromones and the results of their interaction can be also encoded using RGB color.

II. ARTIFICIAL PHEROMONE COMMUNICATION

COS Φ (Communication System via Pheromone) is a high precision, flexible and low-cost experimental setup, which provides a reliable and user friendly platform to study bio-inspired mechanisms. The proposed system consists of: i) a visual localization system which detects the positions of swarm robots and releases the visual pheromones on the LCD screen and ii) a lightweight (~ 20 g) micro-robot platform with a specific design enables reading the visual pheromone trails using its light sensors.

A. Pheromone Model

The artificial pheromone system simulates several pheromones and their interactions at the same time. The combined effect of the pheromones is displayed on a horizontal LCD screen as a gray-scale image, which is sensed by the robots' light sensors. The system allows each robot to release several pheromones at the same time depending on user-specified conditions, e.g. the distance from a food source or another robot.

The behavior of each pheromone is determined by four parameters:

- injection ι , which defines how fast a particular pheromone is released by a given robot,
- evaporation half-life e_ϕ , that determines how quickly the pheromone strength fades over time,
- diffusion κ , that defines the rate at which the pheromone is spreading,
- influence c , that characterizes how much the pheromone influences the image displayed on the horizontal screen.

Given that the image displayed on the screen is represented as a matrix \mathbf{I} , brightness of a pixel at a position (x, y) is presented as $\mathbf{I}(x, y)$, and an i^{th} pheromone is modeled as a matrix Φ_i , the brightness of each pixel that is displayed on the horizontal screen is given by

$$\mathbf{I}(x, y) = \sum_{i=1}^n c_i \Phi_i(x, y), \quad (1)$$

where $\Phi_i(x, y)$ is a 2D array that represents i^{th} pheromone intensity at location (x, y) and c_i defines the pheromone's influence on the displayed image. Note that the values of c_i can be both positive and negative which allows the individual pheromones not only to increase the displayed pixel's brightness, but also to suppress it.

Strengths of each pheromone are continuously updated by

$$\dot{\Phi}_i(x, y) = \frac{\ln 2}{e_{i\phi}} \Phi_i(x, y) + \kappa_i \Delta \Phi_i(x, y) + \iota_i(x, y) \quad (2)$$

where $\dot{\Phi}_i(x, y)$ corresponds to the rate of the pheromone change caused by its evaporation $e_{i\phi}$, diffusion κ_i and

injection ι_i . The injection $\iota_i(x, y)$ for a particular pheromone i and position (x, y) is determined by a set of conditions that are tied to the positions of the individual robots. Typically, a robot at a particular position would set the injection within a given radius to a particular value, i.e.

$$\iota_i(x, y) = \begin{cases} s_\phi & \text{if } \sqrt{(x - x_r)^2 + (y - y_r)^2} \leq l_\phi/2, \\ 0 & \text{otherwise,} \end{cases}, \quad (3)$$

where (x_r, y_r) is the robot position, l_ϕ is the width of the pheromone trail and s_ϕ is the pheromone release rate.

The system allows to extend the first term of Equation 2 by a linear combination of all simulated pheromones:

$$\dot{\Phi}_i(x, y) = \sum e'_{ij\phi} \Phi_j(x, y) + \kappa_i \Delta \Phi_i(x, y) + \iota_i(x, y). \quad (4)$$

The parameters $e'_{ij\phi}$ in Equation 4 define how the strength of j^{th} pheromone affects the i^{th} pheromone rate of change, which corresponds to modeling the pheromone's interaction as a linear dynamical system. Since the pheromones released by different robots can have different evaporation and diffusion rates and can strengthen or suppress each other, their interactions with the robots can result in a complex swarm behavior.

B. Localization system

The localization system is based on a freely available software package capable of fast and precise tracking of a large number of black-and-white patterns that are placed on the robots. The core of the localization system [19] is a method that can detect a black and white roundel consisting of two concentric annuli with a white central disc [20]. The authors claim that the localization precision is in the order of millimeters and the system is able to track hundreds of patterns in real-time. In order to make the system applicable for our purposes, we had to extend it by:

- adding an automatic calibration step that allows to quickly establish the transformation between the camera and arena coordinate systems,
- changing the circular patterns to elliptical so that the orientation of the robots can be established,
- modifying the patterns so that the individual robots can be distinguished from each other.

In order to make the system setup convenient and quick, we have implemented a self-calibration procedure that allows to automatically establish the relation between the image and real-world coordinates. The procedure takes less than 3 seconds and is automatically performed at the beginning of each experiment. The purpose of the auto-calibration is to prevent the loss of localization precision in case that the experiment preparation procedure (accidentally) affects the relative position of the localization camera and the display. During auto-calibration, the system shows four circular patterns in known positions at the corners of the screen. This allows to establish the transformation between the image coordinates of the patterns and robot positions within the arena. The transformation between these two coordinate systems is performed by means of homography.

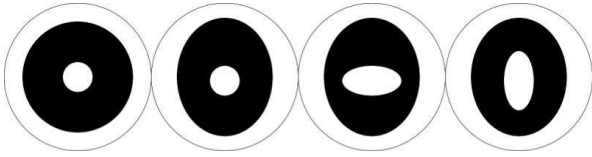


Fig. 2. One original (left) and three modified localization patterns.

When establishing the parameters of the homography, the system takes into account that the calibration patterns are located in a different height than the patterns on top of the robots. This corrective step requires that the robots in the arena have the same height and that intrinsic parameters of the camera are known.

C. Circular pattern modifications

The original system [19] allows to track multiple patterns and calculates their 3D positions, but it does not distinguish between them and does not provide their orientations. However, evaluation of the swarm experiments requires to distinguish between the individual robots and to calculate their orientation.

Thus, we changed the pattern shape from a circle to an ellipse with dimensions of 32×26 mm and shifted the center of the inner white circle by 1 mm, so that the patterns are not concentric any more. The orientation of the pattern's major axis allows to establish the orientation of the robot within $[-90^\circ, 90^\circ]$ and the relative positions of the outer and inner circles' centers allow to resolve the orientation ambiguity.

Moreover, we changed the inner, white patterns from circles to ellipses as well. The dimensions of the inner pattern now encode the pattern ID, which allows to distinguish between the individual robots on the arena. Comparison of the original pattern of [19] and our modified ones is given in Fig. 2.

D. Localization system speed

While processing the camera image to obtain the positions of the robots took less than $50 \mu\text{s}$ per robot, we noticed a delay between the actual robot position and the position of the released pheromone. When a pheromone-releasing robot performs quick movements, this delay causes the pheromone not to appear directly under the center of the robot, but a few millimeters behind it. We assume that this delay is caused by the time needed to transfer the image through the USB interface, communication overhead between the localization and pheromone system and GUI-related calculations. Despite of the delay, the pheromone is still injected under the robot's base and the aforementioned effect does not affect the experiments.

III. EXPERIMENTAL SETUP

A. Robotic Platform

We used *Colias-Φ* micro-robot which is an extended version of *Colias* robot [21]. It is specially designed for swarm robotic applications with very compact size of 4 cm

as shown in Fig. 4(a). The robot has two micro DC gear-head motors each connected to a wheel with diameter of 2.2 cm. The rotational speed for each motor is controlled individually using pulse-width modulation [22]. Each motor is driven separately by an H-bridge DC motor driver, and draws an average current of 35 ± 5 mA in no-load and up to 150 ± 20 mA in stall conditions.

The robot employs three short-range IR proximity sensors to detect and avoid obstacles within a distance of approximately 2 ± 0.5 cm [23]. Power consumption of the robot with forward motion (in a quiet arena with only walls) is about 800 mW. A 3.7 V, 600 mAh lithium-polymer battery is used as the main power source, which allows for 2 hour-long continues operation.

Colias-Φ uses the similar architecture with the original *Colias* with two changes: i) it does not have the IR (long- and short-ranges) communication modules and ii) the lower board is equipped with 5 light intensity sensors that are faced to the LCD screen as shown in Fig. 4(b). These sensors read the intensity of light (I_{s_i} , where i refers to the position of the sensor at the bottom of the robot) varying linearly from 0 and 255.

B. Robot Behavior

Observations of trail follower ants showed that their trail-following behavior is fault tolerant and robust as shown in Fig. 3. The trail following ant moves on a curve to the left until its right antenna detects the pheromone trail, then the ant continues its motion with a turn to the right until its left antenna detects the pheromone trail [6].

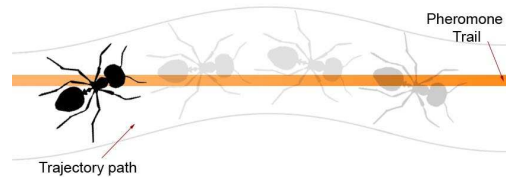


Fig. 3. Trajectory of ants for following the pheromone trail.

We resort a similar approach seen in trail follower ants. *Colias-Φ* when following a trail formed by artificial pheromones controls its left and right motors based on light intensity readings from the left (I_L) and right (I_R) sensors. These two sensors act as if they were ants' antennas. The robot tries to keep its position on a pheromone trail by changing the rotational speeds of its left and right motor. The rotational speeds are calculated as:

$$N_L = \frac{I_L - I_R}{\alpha} + u, \quad (5)$$

$$N_R = \frac{I_R - I_L}{\alpha} + u, \quad (6)$$

where I_L and I_R are the readings (between 0 and 255) from the left and right sensors, u is a biasing speed and α is the rotational speed sensitivity coefficient. The rotational speed coefficient is tuned empirically to have a smoother motion.

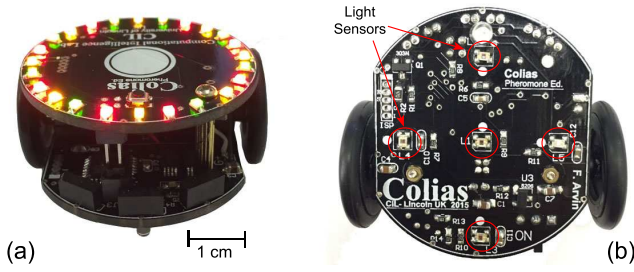


Fig. 4. (a) Colias- Φ mobile robot. (b) Lower board of the robot and light sensors.

TABLE I

EXPERIMENTAL VALUES OR RANGE FOR VARIABLES AND CONSTANTS

Values	Description	Range / Value(s)
n_s	Population size	{3, 6} robots
I_s	Sensor reading of illuminance	0 to 255
u	Robot forward velocity	5 cm/s
N	Rotational speed of motors	0 to 80 rpm
e_ϕ	Evaporation half-life of pheromone trail	{2, 5, 10} sec
κ	Diffusion coefficient	0
R_ϕ	Number of robots on pheromone trail	0 to 5 robots
R_f	Number of robots with random walk	0 to 5 robots
d_r	Distance of a robot from leader	0 to 100 cm
l_ϕ	Pheromone trail width	30 mm
ξ	Consistency of swarm	5 to 100 cm
T	Duration of experiments	150 sec
t	Time	0 to 150 sec

C. Arena Configuration

To implement COS Φ , we use a rectangular arena with a size of 93×52 cm². We use a full HD 42" LCD screen as the ground (as shown in Fig. 1). A very useful feature of Colias- Φ is the light (illuminance) sensors faced to the bottom side of the robot which gives an opportunity to use a LCD flat screen as the ground, see Fig. 4b. Therefore, the pheromone-based swarm scenarios with complex and dynamic environments interactions can be simply implemented on the flat LCD screen. In our experiments, pheromone trails are displayed with a maximum illuminance of 420 lux and the system is controlled by a desktop PC.

D. Experimental Setup

To evaluate the performance of the COS Φ , we used two different setups. One is the single-robot scenario to measure the precision of the system and the other is the swarm scenario to measure how the system performs in a multi-robot setting. Each experiment repeated 6 times and all results are illustrated as box-plots. In the box-plots, boxes show the range of the first and the third quartiles of the data. Median of the data is shown with a horizontal line inside the boxes. Vertical lines (whiskers) show the range between the minimum and maximum of the data.

The standard values of the constants and variables, which are used in this study are listed in Table I.

1) *Single-robot Scenario*: In this scenario, three different pheromone trails are displayed on the LCD screen at a time and a single Colias- Φ robot is used to follow these trails. Two of these pheromone trails are set to be circles with different



Fig. 5. Localization precision experiment: A snapshot of the experiment with Colias- Φ robot following a complex path. (LCAS stands for the Lincoln Centre of Autonomous Systems)

diameters and the last trail is a very complex shape shown in Fig. 5.

2) *Swarm Scenario*: We implement a basic swarm scenario with Colias- Φ robots. In this scenario, follower robots move randomly and when they detect a pheromone trail, they follow this trail. The pheromone trail, which is a high-brightness constant width (l_ϕ) line, is laid by the leader robot. The leader robot moves forward with a constant speed of u in a random direction. When a follower robot detects a pheromone trail, it chooses a random direction (left or right) to follow the trail. Robots join the pheromone with probability of p_{join} and leave the trail occasionally with a probability of p_{leave} . We assume $p_{leave} = 0$ in the scenario, however there are several parameters which change the p_{leave} such as the noise in the reading of the light intensities, collisions with other robots which results in an unexpected turns and overcrowding in a part of arena which pushes the robots to leave the pheromone.

In all the swarm scenario experiments, we used one leader and different number of followers and different evaporation half-life. In particular, we adopted two different configurations: (1) 1 leader, 2 followers and evaporation half-life of 2, 5, 10. (2) 1 leader, 5 followers and evaporation half-life of 5, 10. The number of robots which are following the pheromone trail were counted in every 10 sec intervals.

E. Metrics

1) *Single-robot Scenario*: We use two different metrics for the single robot and the swarm scenario. In the single robot scenario, we use a localization error metric (ϵ_1) for the two circular pheromone trails defined as:

$$\epsilon_1 = \frac{1}{n} \sum_{i=1}^n |\sqrt{(x_i - x_c)^2 + (y_i - y_c)^2} - r|, \quad (7)$$

where x_c and y_c are the coordinates of the circular path's center and r is its diameter. The x_i and y_i denote the positions of the robot measured over time and n is the total number of measurements taken.

The third, more complex path cannot be defined analytically, but it is a sequence of points denoted as (x_p, y_p) . In that case, the localization error ϵ_2 is calculated as an average distance of the robot position from the path as:

$$\epsilon_2 = \frac{1}{n} \sum_{i=1}^n \min \sqrt{(x_i - x_p)^2 + (y_i - y_p)^2}. \quad (8)$$

2) *Swarm Scenario*: We use two metrics in the swarm scenario. One is the number of robots following the pheromone trail (R_ϕ) at any instant and the other is the consistency of the swarm, which is average distance of the swarm robots from the leader (d_r).

Number of robots following the pheromone trail is calculated by implementing a simple vision algorithm using the tracking system. The consistency metric is calculated by taking the average of the Euclidean distance of each robot from the leader as:

$$\xi(t) = \frac{1}{n_s} \sum_{i=1}^{n_s} d_{r_i}(t), \quad (9)$$

IV. RESULTS

In this section, we explain the observed results from the pheromone communication system focusing on the individual and group behavior of the robots.

A. Single-robot Scenario

In all three cases, the localization error ϵ_1 and ϵ_2 were less than 1 mm, which is satisfactory for our purposes. Note that the ϵ calculated by (7) and (8) actually encompasses both localization system error and the robot's path following imprecision. Given that $\epsilon \leq 1$ mm, the aforementioned experiments also demonstrated that the robots are able to follow the given paths with a good precision.

B. Swarm Scenario

Prior to performing the experiments related to the swarm scenario, we first evaluated the accuracy and feasibility of the localization system in tracking and pheromone trail releasing. In addition, the robots' ability to follow the pheromone trail was also investigated. Fig. 6 shows the trajectory of three robots in a randomly selected experiment. The thick grey line indicates the pheromone trail on the LCD screen which is the trajectory of the leader robot. Two dashed lines are the trajectories of the follower robots. The positions of the robots reveal that the two followers were able to follow the leader without any explicit direct communication (or neighboring position estimation) system.

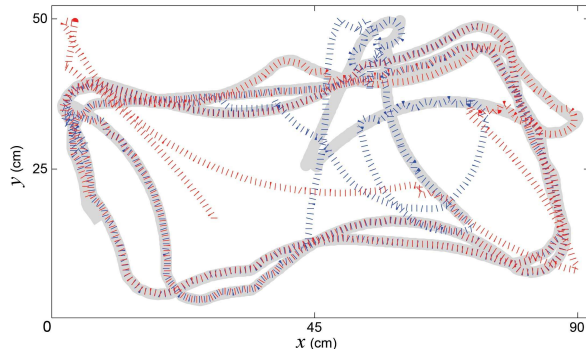


Fig. 6. Trajectory of a leader (grey shadow) and two robots (dashed lines with red and blue colours) in a randomly selected experiment ($e_\phi = 10$ sec).

The results of the experiment with three robots –one leader and two followers–, depicted in Fig. 7 show that the increase in the evaporation half-life resulted in increase the number of follower robots on the pheromone trail. In higher evaporation half-life, pheromone trail lasts longer than the lower evaporation half-life. Therefore, the chance of the followers to meet the pheromone trail increases by increasing the e_ϕ . Moreover, the results also reveal that the number of robots increases with time except in the $e_\phi = 2$ sec. case. In the 2 sec case, robots occasionally join and leave the pheromone trail due to shorter pheromone trail length, hence number of robots never stabilizes at a certain value.

Fig. 8 shows the number of robots during experiments with six robots – one leader and five followers. We only investigate the effects of two evaporation half-life ($e_\phi \in \{5, 10\}$ sec) and eliminated the experiments with $e_\phi = 2$ sec due to the short pheromone trail which can not accommodate 5 followers in the same time. Similar to the previous configuration, increasing the evaporation half-life, increases the tendency of the robots to follow the pheromone trail. We can also observe that the system reaches steady-state faster when the evaporation half-life is 10 sec.

Fig. 9 shows the distance of robots during experiments with 3 and 5 robots. We analyzed the experiments with the longest evaporation half-life ($e_\phi = 10$ sec). The results showed that, consistency of the group increases with time.

V. DISCUSSION AND CONCLUSION

We presented a novel artificial pheromone communication system, COS Φ , as a low-cost and reliable laboratory experimental setup to be used in bio-inspired swarm robotic researches. The system consists of a low-cost open-hardware micro robot and an open-source localization system which tracks the robots trajectory and releases the artificial pheromone. We tested the system in an exploration scenario with a group of *Colias- Φ* micro robots. We made several observations:

- Increase in evaporation half-life, increases the stability of the pheromone trail, hence increases the chance of a follower to find and follow that trail as discussed in [4], [17].
- Since, we did not define any interaction between the robots, the population size does not impact the consistency in a significant way. However, increasing the number of robots resulted in a slight increase of the individual distances from the leader (Fig. 9) due to more frequent inter-robot collisions.

We can conclude that the proposed system is feasible and convenient for bio-inspired swarm robotics research. For the future work, we will investigate the influence of the diffusion and evaporation rates on the swarm performance and behavior in more complex environments with obstacles.

The source codes of the system described are publicly available [24].

REFERENCES

- [1] E. Şahin, S. Girgin, L. Bayındır, and A. E. Turgut, "Swarm Robotics," in *Swarm Intelligence*, 2008, vol. 1, pp. 87–100.

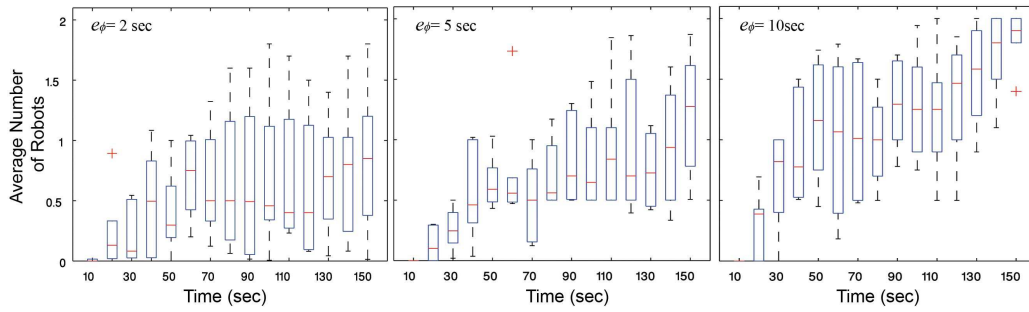


Fig. 7. Average number of robots on the pheromone trail in different evaporation half-life ($e_\phi \in \{2, 5, 10\}$ sec) with 3 robots (one leader and 2 followers).

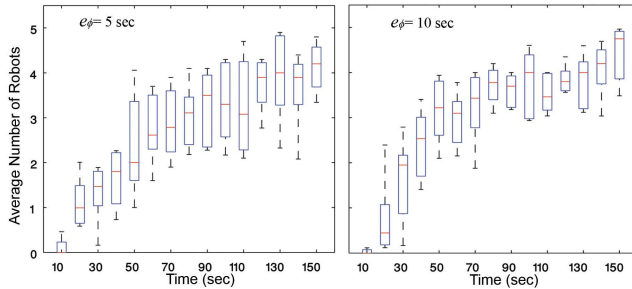


Fig. 8. Average number of robots on the pheromone trail in different evaporation half-life ($e_\phi \in \{5, 10\}$ sec) with 6 robots (one leader and 5 followers).

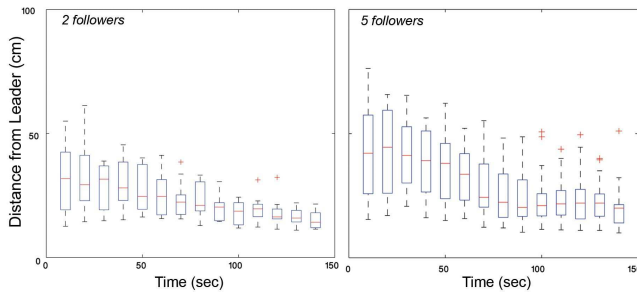


Fig. 9. Distance of each individual follower, d_r , from the leader robot during the experiments with 2 and 5 followers in $e_\phi = 10$ sec.

[2] S. Camazine, N. Franks, J. Sneyd, E. Bonabeau, J.-L. Deneubourg, and G. Theraulaz, *Self-organization in Biological Systems*. Princeton University Press, 2001.

[3] B. Hölldobler and E. O. Wilson, *The Ants*. Harvard University Press, 1990.

[4] F. Fossum, J.-M. Montanier, and P. C. Haddow, "Repellent pheromones for effective swarm robot search in unknown environments," in *IEEE Symposium on Swarm Intelligence (SIS)*, 2014, pp. 1–8.

[5] M. Brambilla, E. Ferrante, M. Birattari, and M. Dorigo, "Swarm robotics: a review from the swarm engineering perspective," *Swarm Intelligence*, vol. 7, no. 1, pp. 1–41, 2013.

[6] R. A. Russell, "Ant trails—an example for robots to follow?" in *IEEE International Conference on Robotics and Automation*, 1999.

[7] A. H. Purnamadajaja and R. A. Russell, "Bi-directional pheromone communication between robots," *Robotica*, vol. 28, no. 01, pp. 69–79, 2010.

[8] R. A. Russell, "Air vortex ring communication between mobile robots," *Robotics and Autonomous Systems*, 2011.

[9] R. Fujisawa, S. Dobata, K. Sugawara, and F. Matsuno, "Designing

pheromone communication in swarm robotics: Group foraging behavior mediated by chemical substance," *Swarm Intelligence*, 2014.

[10] Herianto, T. Sakakibara, and D. Kurabayashi, "Artificial Pheromone System Using RFID for Navigation of Autonomous Robots," *Journal of Bionic Engineering*, vol. 4, no. 4, pp. 245–253, 2007.

[11] A. A. Khaliq and A. Saffiotti, "Stigmergy at work: Planning and navigation for a service robot on an rfid floor," in *IEEE International Conference on Robotics and Automation (ICRA)*, 2015.

[12] F. Arvin, A. Turgut, F. Bazyari, K. Arikan, N. Bellotto, and S. Yue, "Cue-based aggregation with a mobile robot swarm: a novel fuzzy-based method," *Adaptive Behavior*, vol. 22, pp. 189–206, 2014.

[13] O. Holland and C. Melhuish, "An Interactive Method for Controlling Group Size in Multiple Mobile Robot Systems," in *8th International Conference on Advanced Robotics*, 1997, pp. 201–206.

[14] S. Garnier, M. Combe, C. Jost, and G. Theraulaz, "Do ants need to estimate the geometrical properties of trail bifurcations to find an efficient route? a swarm robotics test bed," *PLoS computational biology*, vol. 9, no. 3, p. e1002903, 2013.

[15] F. Arvin, K. Samsudin, A. R. Ramli, and M. Bekravi, "Imitation of Honeybee Aggregation with Collective Behavior of Swarm Robots," *International Journal of Computational Intelligence Systems*, vol. 4, no. 4, pp. 739–748, 2011.

[16] T. Schmickl, R. Thenius, C. Moeslinger, G. Radspieler, S. Kernbach, M. Szymanski, and K. Crailsheim, "Get in touch: cooperative decision making based on robot-to-robot collisions," *Autonomous Agents and Multi-Agent Systems*, vol. 18, no. 1, pp. 133–155, 2009.

[17] K. Sugawara, T. Kazama, and T. Watanabe, "Foraging behavior of interacting robots with virtual pheromone," in *IEEE/RSJ International Conference on Intelligent Robots and Systems (IROS)*, 2004.

[18] S. Garnier, F. Tache, M. Combe, A. Grimal, and G. Theraulaz, "Alice in pheromone land: An experimental setup for the study of ant-like robots," in *Swarm Intelligence Symposium*, 2007, pp. 37–44.

[19] T. Krajník, M. Nitsche, J. Faigl, P. Vaněk, M. Saska, L. Přeučil, T. Duckett, and M. Mejail, "A practical multirobot localization system," *Journal of Intelligent & Robotic Systems*, 2014.

[20] T. Krajník, M. Nitsche, J. Faigl, T. Duckett, M. Mejail, and L. Přeučil, "External Localization System for Mobile Robotics," in *Proceedings of the International Conference on Advanced Robotics (ICAR)*, 2013.

[21] F. Arvin, J. Murray, C. Zhang, and S. Yue, "Colias: An Autonomous Micro Robot for Swarm Robotic Applications," *International Journal of Advanced Robotic Systems*, vol. 11, no. 113, pp. 1–10, 2014.

[22] F. Arvin and M. Bekravi, "Encoderless Position Estimation and Error Correction Techniques for Miniature Mobile Robots," *Turkish Journal of Electrical Engineering & Computer Sciences*, vol. 21, pp. 1631–1645, 2013.

[23] F. Arvin, K. Samsudin, and A. Ramli, "Development of IR-Based Short-Range Communication Techniques for Swarm Robot Applications," *Advances in Electrical and Computer Engineering*, vol. 10, no. 4, pp. 61–68, 2010.

[24] T. Krajník and F. Arvin, "Artificial pheromone system implementation," <http://purl.org/robotics/colias-pheromone>, 2015.